

Evaluation of Hydrogen Sulfide Corrosion Inhibitors for Wet Gas Pipeline Steel

† Vu Dinh Huy¹, Nguyen Thi Phuong Thoa², Tran Quoc Phong²,
and Nguyen Thai Hoang²

¹"Vietsovetro" Joint Venture, 105 Le Loi, vung Tau, Vietnam
²Vietnam National University of Ho Chi Minh City

Wheel test and potentiodynamic polarization methods were used to evaluate the relative effectiveness of some hydrogen sulfide corrosion inhibitors for the wet gas pipeline API 5L grade X 65 steel. Five commercially corrosion inhibitors have been studied in the deoxygenated produced water solutions containing 10 ppm and 100 ppm of hydrogen sulfide. Based on the experiment results the steel corrosion inhibition mechanism is discussed and two most effective corrosion inhibitors are selected.

Keywords : produced water, steel, H₂S, corrosion inhibitors, wheel test, potentiodynamic polarization.

1. Introduction

Corrosion of steel in aqueous environments containing hydrogen sulfide (H₂S) is of great interest in oil and gas industry. The raw gas in "White Tiger" pipeline contains a slight amount of carbon dioxide (CO₂) (less than 0.2% mol) and the actual H₂S concentration is 6-8.5 ppm. The gas is classified as sweet.¹⁾ As a result of temperature and pressure changes along the length of the pipeline water is condensed from produced water in the wet gas phase. Produced water is an extremely complex medium, comprised of liquid water, minerals dissolved from rock formation and water soluble acid gases, such as CO₂ and H₂S. Presence of H₂S even in low concentrations in solutions causes localized corrosion and sulfide stress cracking.²⁾⁻⁴⁾

Inhibitor is the most common way to control internal corrosion in wet gas production pipeline. In the present work H₂S corrosion inhibitors (CI) were evaluated using wheel test and potentiodynamic polarization methods for the API 5L grade X65 steel (X65 steel), which was used to build "White Tiger" wet gas production pipeline.

2. Experimental procedures

2.1 Materials

The Table 1 shows the nominal composition of X65 steel.

Sample dimensions were 50 mm x 20 mm x 3 mm. The specimens were polished in a standard sequence up to 600-grit emery paper, washed in distilled water, and rinsed with acetone. The air-dried specimens were stored in the desiccators 24 hours before the test. The samples were weighed on analytical balance to accuracy of 0.1 mg.

Table 1. The element composition(wt%) of the X65 steel⁵⁾

Element	C _{max}	Mn _{max}	P _{max}	S _{max}	Cb _{min}	V _{min}	Ti _{min}
Content, %	0.26	1.40	0.04	0.05	0.005	0.005	0.005

Table 2. Chemical composition of produced water (density at 24°C 0.9962 g/cm³, conductivity 0.61 mS/cm, pH 7.54, total mineralization 460.0 mg/l, dried remains 124.0 mg/l)

Ion	Cl ⁻	SO ₄ ²⁻	HCO ₃ ⁻	CO ₃ ²⁻	OH	NO ₃ ⁻	Ca ²⁺	Mg ²⁺	Fe ²⁺ Fe ³⁺	Na ⁺ K ⁺
Content, mg/l	41.7	19.9	260.7	0	0	0	3.1	2.4	0.3	132.1

2.2 Test solutions

The produced water was separated from white hydro-

† Corresponding author: vdh@vjv.co.vn

carbon condensate - produced water mixtures. Its chemical composition is given in Tabel 2.

The first testing medium is a solution of 10 ppm H₂S in deoxygenated produced water (1st bland solution). The second one is a solution of 100 ppm H₂S in deoxygenated produced water (2nd blank solution).

five corrosion inhibitors signed as A, B, C, D and E were tested. Solutions of 1% each of them in suitable solvents were prepared.

2.3 Wheel corrosion test^(4),6)

Standard wheel weight loss experiments were run to determine the average corrosion rate of X65 steel in various concentrations (5, 10, 15 and 20 ppm by volume) of CIs.

Purge the air space in the test bottles with nitrogen gas for two hours, and then CIs have been injected. Add the first or second deoxygenated blank solution to total volume of 200 ml. One weighed specimen was placed in each bottle and the latter was welded by resin immediately to avoid air contamination. Test bottles were set on the wheel, which rotated at 26 rpm for 24 hours at temperature 30 ± 1 °C. At the end of the test the bottles were uncapped and steel specimens were removed, cleaned, dried and reweighed. Oxygen contamination in the test solutions was checked after each experiment and found to be negligible.

The weight loss of the test specimens was determined according to the ASTM standards G1-90 and G31-72.^(7),8)

Corrosion inhibition efficiency (IE) was evaluated in terms of percent from average corrosion rates of the steel in test solutions with (V) and without (V₀) addition of corrosion inhibitors by following equation:

$$E(\%) = \frac{V_0 - V}{V_0} \times 100 \quad (1)$$

The average corrosion rate in mm/year(V) was calculated from weight loss data as follows:

$$V(mm/y) = \frac{K \times Weightloss(g)}{Density(g/cm^3) \times cm^2 \times Time(hour)} \quad (2)$$

Where constant K = 8.76 x 10⁴.

2.4 Potentiodynamic polarization measurements

Electrochemical measurements were carried out using a potentiogalvanostat PGS-HH6. Cathodic and anodic polarizations were conducted on X65 steel in the first and the second blank solutions with and without addition of CIs in accordance with ASTM standard G5-94.⁽⁹⁾

Steel samples were polished mechanically with 200 grit to 600-grit paper, cleaned in ethanol, rinsed with distilled

water, dried and mounted in Specifix-20 resin. the round working surface of 1 cm² area was left uncovered. Before each potentiodynamic measurement the working area was polished with emery papers, degreased with ethanol, rinsed in distilled water and dried in cool air. Counter electrode was a platinum string with the surface area of 9 cm², reference electrode was a saturated calomel electrode (SCE) placed in a separate compartment.

In the high overpotential range the polarization was undertaken from the rest potential to the cathodic -250 mV and to anodic 250 mV potentials at the rate of 1.0 mV/s. In the low overpotential range (± 20 mV vs. the rest potential) it was performed from cathodic to anodic potentials at the rate of 0.5 mV/s. All experiments were carried out in the nitrogen environment.

Corrosion current density (*i_{corr.}*) values were calculated by Stern-Geary equation (3):

$$i_{corr.} = \frac{b_a \times b_c}{2.3 \times (b_a + b_c) \times R_p} \quad (3)$$

Where polarization resistance, *R_p* (ohm.cm²), and Tafel slope of the anodic and cathodic curves, *b_a* and *b_c* (mV/decade) were determined using linear polarization resistance and Tafel extrapolation methods according to the ASTM standards G 102-89 and G 59-91.^(10),11)

3. Results and discussion

3.1 X65 Steel corrosion rate obtained by wheel test

The average corrosion rates of X65 steel in the 10 ppm H₂S deoxygenated solutions obtained by the wheel test after 24-hour exposure at 30 °C were shown on Table 3 and Fig. 1.

It was clear from these data that the X65 steel corrosion rate decreased with increasing of CI concentration from 0 to 20 ppm. In consequence, the steel corrosion IE of all studied inhibitors increased with increasing their concentration (Table 4 and Fig. 2).

Table 3. Corrosion rate of the X65 steel in the 10 ppm H₂S deoxygenated solutions obtained by wheel test (wheel speed: 26 rpm, temperature: 30 °C, exposure time: 24 hours)

CI concentration, ppm	Steel corrosion rate, mm/y				
	A	B	C	D	E
0	0.091	0.091	0.091	0.091	0.091
5	0.023	0.03	0.033	0.046	0.044
10	0.021	0.028	0.029	0.043	0.032
15	0.020	0.022	0.023	0.040	0.024
20	0.016	0.018	0.019	0.019	0.023

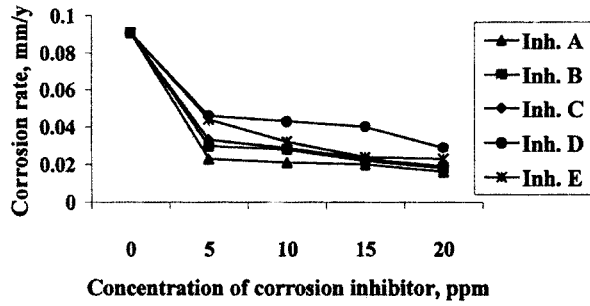


Fig. 1. Effect of corrosion inhibitor concentrations in the 10 ppm H₂S deoxygenated solution on X65 steel corrosion rate.

Table 4. Inhibition efficiency for X65 steel corrosion in the 10 ppm H₂S solution obtained by wheel test

Concentration of CI, ppm	Corrosion inhibitor efficiency, %				
	Inh. A	B	C	D	E
0	0	0	0	0	0
5	74.73	67.03	63.74	49.45	51.65
10	76.92	69.23	68.13	52.75	64.84
15	78.02	75.82	74.73	56.04	73.63
20	82.42	80.22	79.12	68.13	74.73

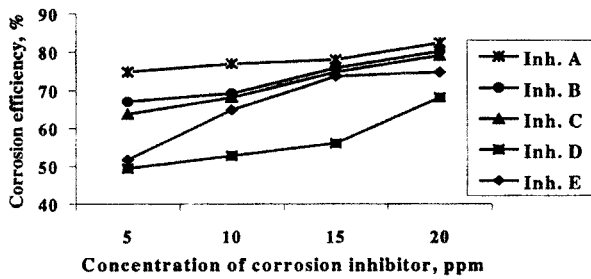


Fig. 2. Concentration dependence of inhibition efficiency for X65 steel corrosion in the 10 ppm H₂S solution.

Table 5. Corrosion rate of the X65 steel in the 100-ppm H₂S deoxygenated solution obtained by wheel test (wheel speed: 26 rpm, temperature 30 °C, exposure time: 24 hours)

Concentration of CI, ppm	Steel corrosion rate, mm/y				
	Inh. A	B	C	D	E
0	0.097	0.097	0.097	0.097	0.097
5	0.075	0.078	0.079	0.088	0.082
10	0.067	0.068	0.070	0.073	0.072
15	0.050	0.052	0.059	0.062	0.060
20	0.028	0.040	0.050	0.058	0.053

The same corrosion inhibitor concentration effect on X65 steel average corrosion rate was observed in the wheel

Table 6. Inhibitor efficiency for X65 steel corrosion in the 100 ppm H₂S deoxygenated solution obtained by wheel test (wheel speed; 26 rpm, temperature: 30 °C, exposure time: 24 hours)

Concentration of CI, ppm	Corrosion inhibitor efficiency, %				
	Inh. A	B	C	D	E
0	0	0	0	0	0
5	22.68	19.59	18.56	9.28	15.46
10	60.93	29.9	27.84	24.74	25.77
15	48.45	46.39	39.18	36.08	38.14
20	71.13	58.76	48.45	40.21	45.36

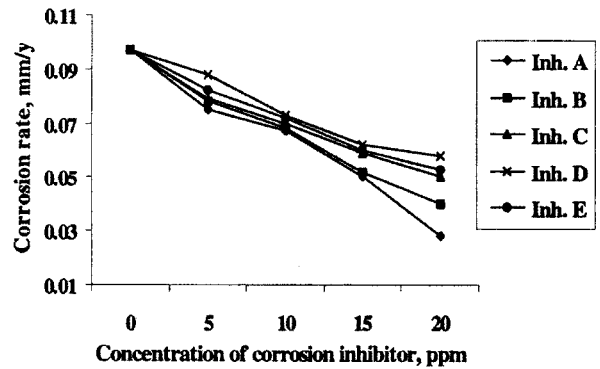


Fig. 3. Effect of corrosion inhibitor concentrations on X65 steel corrosion rate in the 100 ppm H₂S deoxygenated solution.

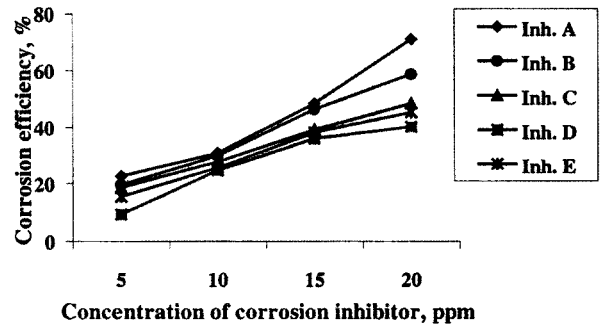


Fig. 4. Concentration dependence of inhibition efficiency for X65 steel corrosion in the 100 ppm H₂S solution.

test for the 100 ppm H₂S deoxygenated solutions (Tables 5, 6 and Figs. 3, 4).

As it was shown by comparison with data in Tables 3, 4 and Figs. 1, 2, when H₂S concentration increased by ten from 10 to 100 ppm, the IE of inhibitors A and B decreased to 15-20 %, For the inhibitors C, D and E this reducing effect was even greater, especially in solutions with low concentration of CI. Furthermore, with increasing H₂S concentration to 100 ppm the localized corrosion

penetration and the embrittlement for X65 steel were observed in the solution containing less than 10 ppm of CIs.

The ranking of studied CIs based on their reductin effect on the X65 steel corrosion rate in rotated deoxygenate solutions containing 10 and 100 ppm H₂S, is as follows:

$$A > B > C > E > D \quad (4)$$

3.2 Electrochemical measurements

Some of anodic and cathodic polarization curves on X65 steel in static deoxygenated 10 ppm H₂S solution in the absence and presence of CIs are shown in Fig. 5 and 6. Electrochemical parameters derived from these curves are given in Table 7.

The corrosion IE values calculated from i_{corr} determined by potentiodynamic measurements in static solutions were lower than those obtained by 24 hours imersion wheel test (compare Table 4 and Table 8, column Inhibition Efficiency). It was suggested that one cause for this difference in IE might have been the difference in experimental

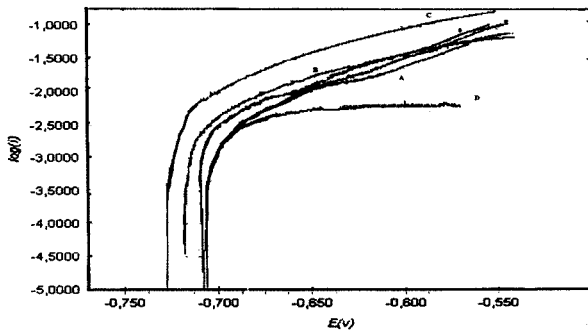


Fig. 5. Anodic polarization curves on the X65 steel in the static deoxygenated 10 ppm H₂S solution (curve 0) containing 20 ppm of A, B, C, D and E inhibitors.

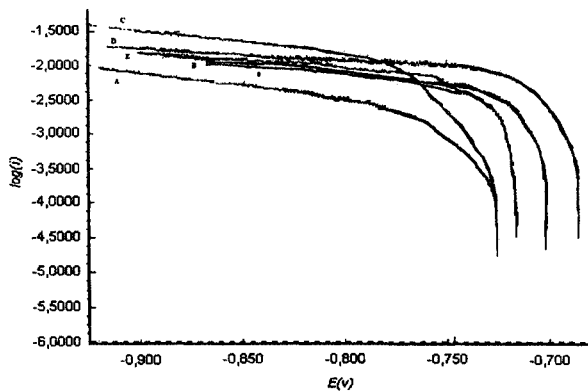


Fig. 6. Cathodic polarization curves on the X65 steel in the static deoxygenated 10 ppm H₂S solution (curve 0) containing 20 ppm of A, B, C, D and E inhibitors.

Table 7. Potentiodynamic polarization parameters of X65 steel corrosion process in static deoxygenated 10-ppm H₂S produced water solutions containing various concentrations of corrosion inhibitors

CI concentration, ppm	-E _{corr} , mV	R _p , ohm·cm ²	b _a , mV	b _c , mV	i _{corr} × 10 ³ , mA/cm ²	Inhibition Efficiency, %	
Blank solution	710	2862	135	440	15.68		
A	5	700	12813	198	320	11.44	20.2
	10	720	14869	330	334	5.96	61.9
	15	708	25754	560	355	4.08	73.8
	20	708	52243	857	360	3.36	76.2
B	5	714	6096	173	365	12.70	19.1
	10	708	14177	200	362	6.90	56.0
	15	710	16240	302	360	5.60	64.3
	20	720	45265	307	256	4.11	73.8
C	5	742	4770	207	485	13.06	16.7
	10	737	5700	210	470	9.52	39.3
	15	730	11215	232	475	6.35	59.5
	20	721	15000	230	500	4.47	71.4
D	5	713	11375	320	468	13.63	13.1
	10	700	12993	1350	489	9.89	36.9
	15	718	16795	1911	434	7.65	51.2
	20	716	19340	1530	344	6.31	59.8
E	5	703	5834	177	458	14.19	9.5
	10	711	6907	198	462	12.54	20.3
	15	700	8000	186	467	9.72	38.1
	20	717	8510	217	392	7.13	54.7

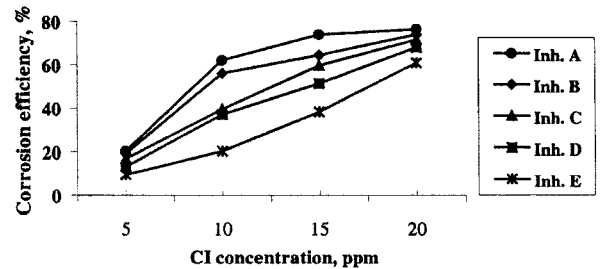


Fig. 7. X65 steel corrosion IE as a function of inhibitor concentration in static deoxygenated 10-ppm H₂S solutions, obtained by potentiodynamic polarization

conditions for these methods. Thus, the steel corrosion IE of studied inhibitors may depend on the solution flowing speed and the exposure time.

R_p significantly increased with increasing inhibitor concentration, especially in the case of A, B and D inhibitors. Moreover these inhibitors increased the anodic Tafel slope (b_a) more considerably than C and E.

Corrosion potential (E_{corr}) and the Tafel slope of cathodic reaction (b_c) remained almost unchangeable in the presence of the inhibitors.

From these results it may be concluded that the studied

inhibitors adsorb on the steel surface and protect it by blocking effect. Inhibiting effect on anodic reaction of steel corrosion process was greater for A, B and D inhibitors.

Corrosion IE as a function of the inhibitor concentration in static 10-ppm H₂S solutions is presented in Fig. 7. In these solutions corrosion IE obtained by electrochemical measurements reduce in the rank:

$$A > B > C > D > E \quad (5)$$

4. Conclusions

1. The X65 steel corrosion rate increased with increasing concentration of hydrogen sulfide in the produced water solutions.

2. The steel corrosion inhibition efficiency increased with increasing concentration of the studied corrosion inhibitors in the test solutions.

3. The inhibition effect of the inhibitors is due to their adsorption on steel surface. The most effective inhibitor for X65 steel corrosion in produced water containing H₂S is A. The second one is inhibitor B. In the presence of these two inhibitors the polarization resistance of X65 steel corrosion process grows up nearly by a factor of 20.

4. The inhibitors A, B and especially D show a greater inhibition effect on the anodic reaction of steel corrosion process than on the cathodic one. D seems to be an anodic inhibitor while C may be classified as a complex inhibitor.

5. The final selection of corrosion inhibitors depends

on other factors such as toxicity, compatibility with other chemicals, and cost.

References

1. Hoang Dinh Tien, Nguyen Thuy Quynh, Ho Trung Chau, and Vu Hoang Long. *J. of Oil & Gas*, **4**, 13 (2001), in Vietnamese.
2. X. Y. Zhang and Y. L. Du, *British Corrosion J.*, **33**(4), 292 (1998).
3. R. Rubiandini and R. S. A. Septiantor, *The 10th Asia-Pacific Corrosion Control Conference Proceedings Book*, pp.G12.1/13-G12.13/13, Bali-Indonesia, 27-31 October (1997).
4. E. Buck, *Corrosion tests and standards: Application and interpretation*, R. Baborian, ed.), p.403, ASTM manual series: MNL 20, USA, 1995.
5. A. Trouvay and B. Cauvin, *Piping Equipment Material Petrole*, Ed. C. Janvier, pp.1-53, 1993.
6. B. F. Davis. *Materials performance*, **21**(12), p.45 (1982).
7. ASTM G1-90: *Standard practice for preparing, cleaning and evaluating corrosion test specimens.*
8. ASTM G31-72: *Standard practice for laboratory immersion corrosion testing of metals.*
9. ASTM G5-94: *Standard reference test method for making potentiostatic and potentiodynamic anodic polarization measurements.*
10. ASTM G102-89: *Standard practice for calculation of corrosion rates and related information from electrochemical measurements.*
11. ASTM G59-91: *Standard practice for conducting potentiodynamic polarization resistance measurements.*